Pathology International 2003; **53**: 106–110

Case Report

Primary carcinosarcoma of the vagina

Rie Shibata,[1] Akihiro Umezawa,[1] Kyoko Takehara,[2] Daisuke Aoki,[2] Shiro Nozawa[2] and Jun-ichi Hata[1,3]

Departments of [1]Pathology and [2]Obstetrics and Gynecology, Keio University School of Medicine, and [3]National Research Institute for Child Health and Development, Tokyo, Japan

Primary carcinosarcoma of the vagina is a very rare tumor, with only eight cases diagnosed as carcinosarcoma in the literature that we are aware of. We recently encountered a case of primary carcinosarcoma of the vagina in a 75-year-old woman. The patient had a history of hysterectomy and bilateral ovariectomy for uterine corpus cancer at 55 years of age. Recurrence of the cancer was suspected 17 years after the operation and irradiation therapy was performed, but the patient died 3 years after the recurrence. Autopsy revealed a mass lesion in the pelvic cavity that originated in the vagina. Histological examination showed that the tumor contained anaplastic carcinoma, rhabdomyosarcoma, leiomyosarcoma and chondrosarcoma components, and it was diagnosed as carcinosarcoma. The histological diagnosis of the uterine corpus cancer was well-differentiated adenocarcinoma, and there was no sarcomatous component. The carcinosarcoma occurred 17 years after the hysterectomy, and it was concluded to be a primary carcinosarcoma of the vagina. This is the first case of primary vaginal carcinosarcoma in which the epithelial and sarcomatous components were clearly identified histologically and immunohistochemically.

Key words: carcinosarcoma, malignant mixed mullelian tumor, vagina.

Carcinosarcomas (malignant mixed mullerian tumors) of the female genital tract are highly aggressive neoplasms characterized by mixture of malignant epithelial and stromal elements. Carcinosarcoma of the uterine corpus is well known, but it accounts for only 2–3% of all malignant tumors of the uterus.[1] Primary carcinosarcoma of the vagina is a very rare tumor, and there are only a few reports of cases diagnosed as carcinosarcoma or malignant mixed mullerian tumor of vaginal origin in the literature.[2–6] We report here a case of primary carcinosarcoma of the vagina that occurred in a 75-year-old woman.

Correspondence: Jun-ichi Hata, National Research Institute for Child Health and Development, 3-35-31 Taishido Setagaya-ku, Tokyo 154-8567, Japan. Email: jhata@nch.go.jp

Received 5 July 2002. Accepted for publication 13 September 2002.

CLINICAL SUMMARY

The patient had a history of hysterectomy and bilateral ovariectomy for cancer of the uterine corpus at age 55 years. The tumor was localized in the uterine corpus and showed deep myometrial invasion. It was diagnosed as stage Ic. The histological diagnosis was well-differentiated adenocarcinoma (Fig. 1a). A mass lesion was detected in the pelvic cavity 17 years after the operation and recurrence of the uterine corpus cancer was suspected. Para-aortic lymph node metastasis was also detected. Biopsy specimen of the tumor lesion at the vagina was diagnosed as poorly differentiated adenocarcinoma (Fig. 1b). Pelvic irradiation therapy was performed, but the patient died 3 years after the recurrence was suspected aged 75 years.

PATHOLOGICAL FINDINGS

At autopsy, the tumor was found to have originated in the vagina, directly invading the bladder, and formed a mass lesion in the pelvic cavity. The mass had compressed both ureters, causing hydronephrosis and hydroureter. Bone metastasis and a para-aortic lymph node metastasis were also diagnosed. The para-aortic lymph node to which the tumor had metastasized measured 15 × 9.5 × 11 cm. Its cut surface was white to yellow-white, and necrosis and hemorrhage were observed (Fig. 2).

Histological examination of the pelvic mass lesion at autopsy revealed mainly anaplastic carcinoma (Fig. 3a). The tumor cells contained bizarre nuclei and exhibited high mitotic activity. A small rhabdomyosarcoma component, which was positive for myoglobin (data not shown), was present. Squamous epithelium of the vagina could not be identified because of degenerative changes and necrosis. The metastatic lesion of the para-aortic lymph node contained components consistent with rhabdomyosarcoma (Fig. 4b), leiomyosarcoma (Fig. 4c) and chondrosarcoma (Fig. 4d) as well as anaplastic carcinoma. The metastatic lesion of the bone contained a chondrosarcoma component.

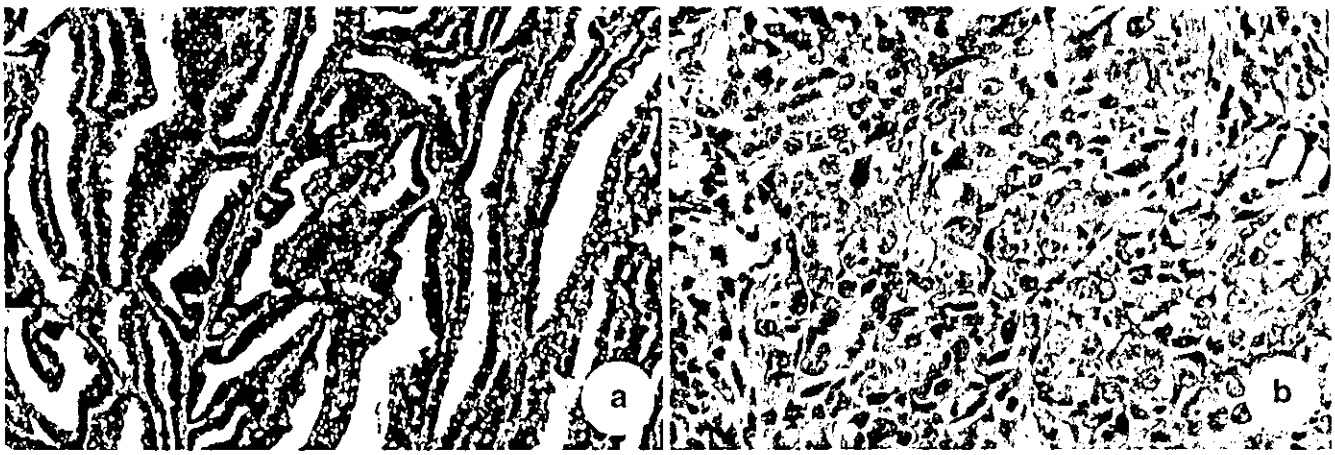

Figure 1 Histological appearance of the uterine corpus cancer at 55 years and the biopsy specimen of the vagina when the pelvic mass was detected 17 years later. (**a**) The histological diagnosis of the uterine corpus cancer was well-differentiated adenocarcinoma and no sarcomatous components were seen. The tumor cells had a glandular pattern and exhibited papillary growth. (H&E, original magnification ×40) (**b**) Biopsy specimen of the vagina. The tumor cells had atypical nuclei and proliferated without a glandular pattern. (H&E, original magnification ×200)

Figure 2 Cut surface of the paraaortic lymph node to which the carcinosarcoma had metastasized. The node measured 15 × 9.5 × 11 cm, and its cut surface was yellow-white in color. The lesion was mainly composed of solid and soft parts, but there were also hard foci. Necrosis and hemorrhage were seen.

Immunohistochemical results are summarized in Table 1. The tumor cells of the anaplastic carcinoma component were positive for broad-spectrum cytokeratin (Fig. 4a). The tumor cells of the rhabdomyosarcoma component were positive for myoglobin (Fig. 4b), the tumor cells of the leiomyosarcoma component were positive for smooth muscle actin (Fig. 4c), and the tumor cells of the chondrosarcoma component were positive for S-100 protein (Fig. 4d). All the tumor cells were negative for neuron-specific enolase, chromogranin and synaptophysin (data not shown).

DISCUSSION

Primary vaginal carcinosarcoma is a very rare tumor, and only eight cases have been reported in the literature.[2-6] Seven cases were in review articles on female genital tract malignancies, but histological and immunohistochemical information on each case was not described in the literature.[2,3,5,6] Neesham *et al.* reported one case of homologous vaginal carcinosarcoma[4] without a detailed account of the immunohistochemical study. Our case is the first case in

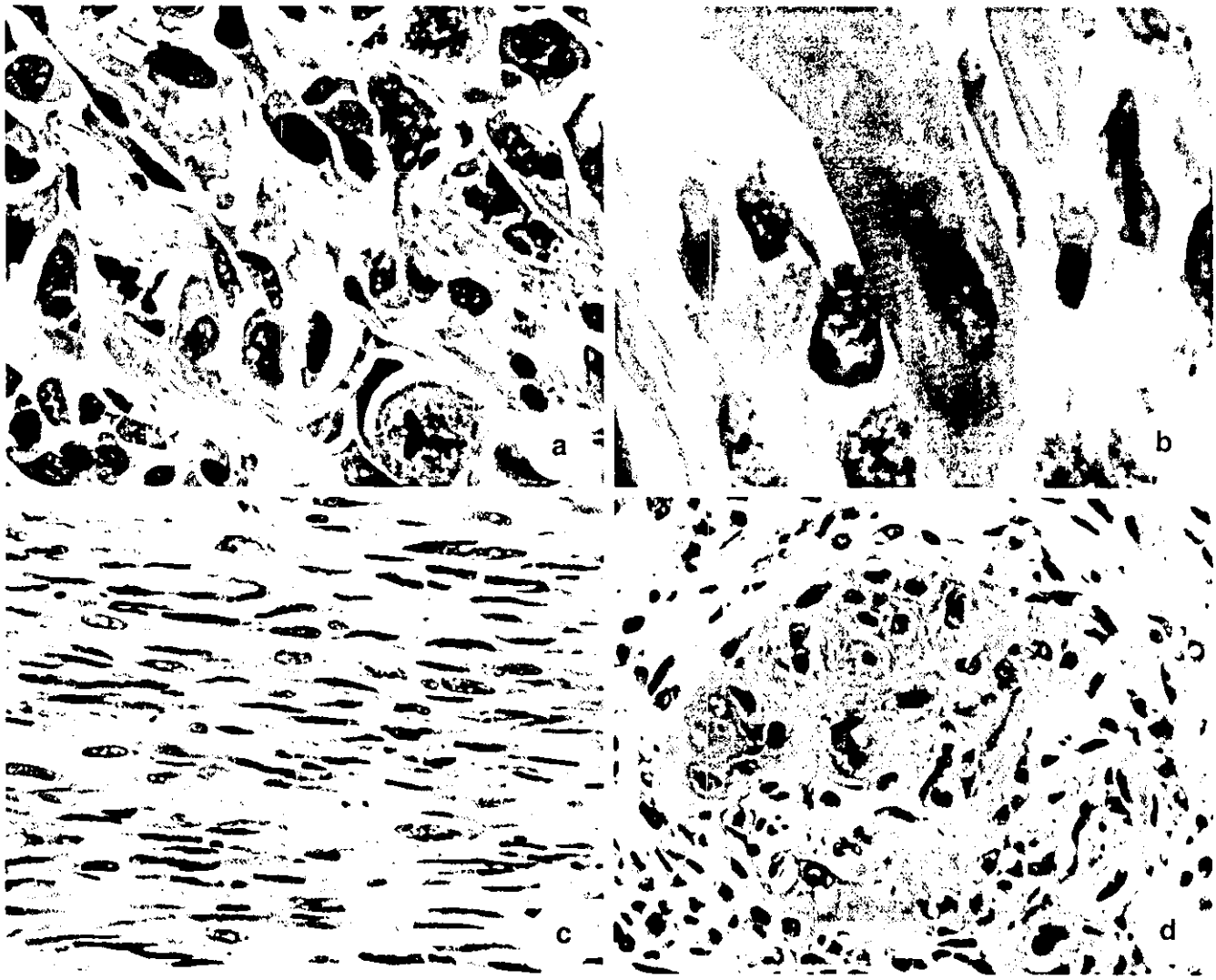

Figure 3 The epithelial and sarcomatous components of carcinosarcoma. (H&E) (**a**) Anaplastic carcinoma. Tumor cells with bizarre nuclei proliferated and atypical mitoses were seen (original magnification ×200) (**b**) Rhabdomyosarcoma. Tumor cell showed striated structure (original magnification ×400) (**c**) Leiomyosarcoma. Tumor cells with spindle-shaped cytoplasm were seen (original magnification ×200) (**d**) Chondrosarcoma. The tumor components formed hyaline cartilage (original magnification ×200).

which epithelial and sarcomatous components have been clearly identified histologically and immunohistochemically. The patient was diagnosed with uterine corpus cancer 20 years before she died, and the histological diagnosis was well-differentiated adenocarcinoma with no sarcomatous component. A pelvic mass was detected 17 years after the hysterectomy, and a biopsy specimen of the vagina was diagnosed as poorly differentiated adenocarcinoma. At first, the tumor was thought to be a recurrence of the adenocarcinoma diagnosed 17 years previously, but at autopsy, the pelvic tumor was found to have originated in the vagina and to be a carcinosarcoma. The biopsy specimen of the vagina 3 years before the patient's death did not represent a recurrence of the adenocarcinoma, but the epithelial component of the carcinosarcoma contained a different neoplasm. As the patient had undergone hysterectomy and bilateral ovariectomy, the carcinosarcoma definitely arose in the vagina.

Recent studies have suggested the combination tumor theory to explain the histogenesis of gynecologic carcinosarcoma.[7,8] Although vaginal carcinosarcoma was not included among the cases, as the proximal portion of the vagina is derived from the mullerian duct, the histogenesis of vaginal carcinosarcomas is thought to be the same as that of uterine carcinosarcomas. Sreenan *et al.* suggested the so-called conversion theory, which could be regarded as a variant of the combination theory.[9] They concluded that the dominant element in carcinosarcomas of the female genital tract is the epithelial component, and sarcomatous components evolve from the carcinoma as a secondary phenomenon. Our case received irradiation therapy after carcinoma of the vagina

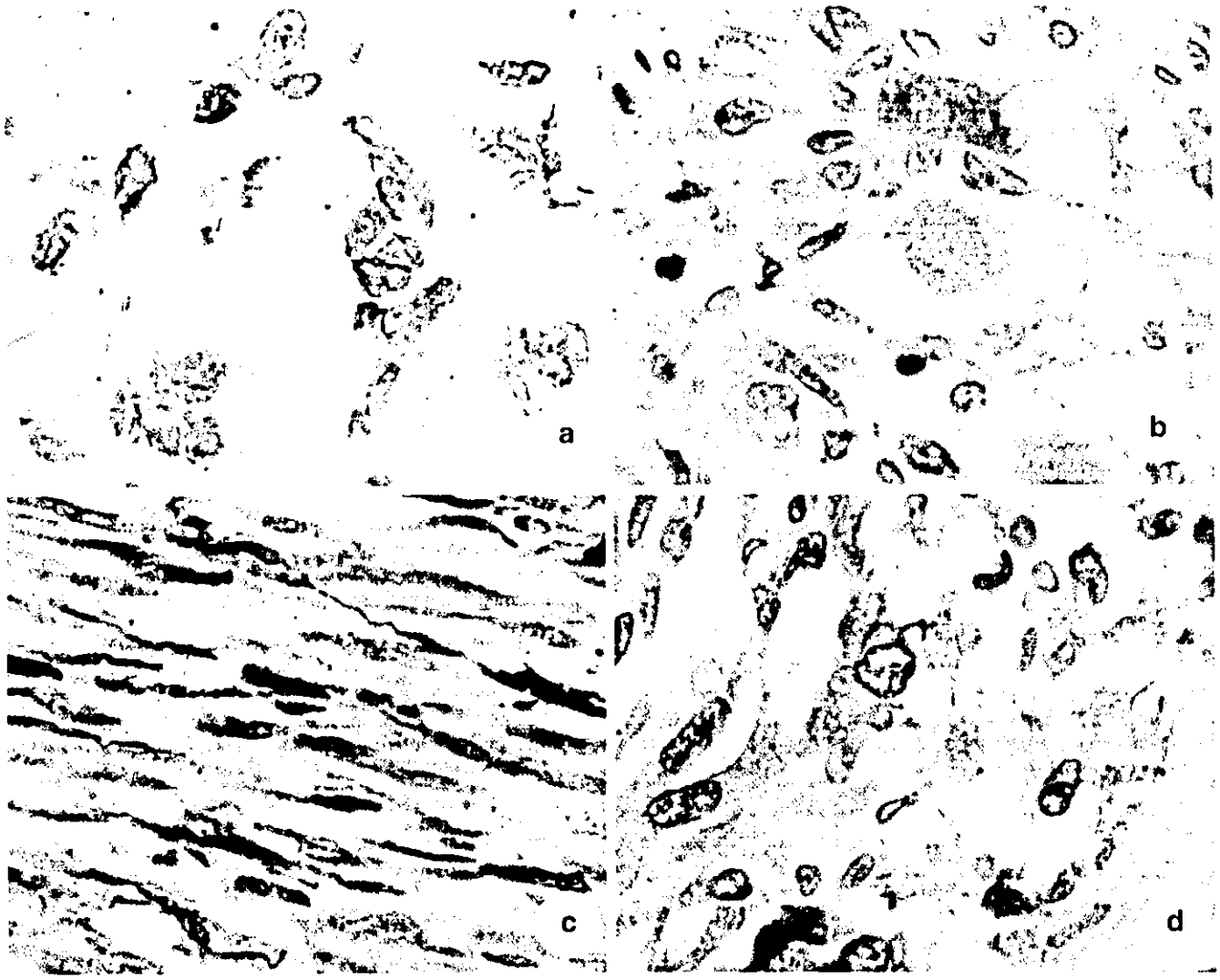

Figure 4 Immunohistochemical analysis of the carcinosarcoma (original magnification ×200). **(a)** The anaplastic carcinoma component is positive for broad-spectrum cytokeratin. **(b)** The rhabdomyosarcoma component is positive for myoglobin. **(c)** The leiomyosarcoma component is positive for smooth-muscle actin. **(d)** The chondrosarcoma component is positive for S-100 protein.

Table 1 Results of immunohistochemical staining

Antigen	Source	Dilution	Carcinoma	Rhabdomyosarcoma	Leiomyosarcoma	Chondrosarcoma
Broad-spectrum cytokeratin	Dako, Kyoto, Japan	1:100	Positive	Negative	Negative	Negative
Myoglobin	Santa Cruz, CA, USA	1:200	Negative	Positive	Negative	Negative
Smooth-muscle action	Santa Cruz	1:100	Negative	Negative	Positive	Negative
S-100	Santa Cruz	1:200	Negative	Negative	Negative	Positive
Neuron-specific enolase	Biogenex, CA, USA	1:2000	Negative	Negative	Negative	Negative
Chromogranin A	Dako	1:200	Negative	Negative	Negative	Negative
Synaptophysin	Dako	1:20	Negative	Negative	Negative	Negative

was detected. It might be possible that irradiation influenced the conversion of carcinoma to sarcoma. Further investigation on the histological changes of carcinosarcomas after irradiation therapy to determine the histogenesis of carcinosarcomas is required.

An association between carcinosarcoma and previous irradiation of the pelvic cavity has been well established.[10] Irradiation therapy was performed in our patient, but it was after development of the carcinosarcoma and the uterine corpus cancer had been treated by surgical resection of uterus and ovaries. Therefore, the patient had no history of chemotherapy or irradiation therapy. The relationship between the adenocarcinoma of uterine corpus and carcinosarcoma of vagina is unclear.

The 5-year survival rate for vaginal carcinosarcoma has been reported to be 17%,[5] and only one case of 5-year survival without disease has been reported.[2] The prognosis of uterine corpus carcinosarocma is also poor, and the reported 5-year survival rate is 18–39%. The outcome of metastatic carcinosarcomas is extremely poor, and Colombi reported that patients died within 1 year of diagnosis.[11] However, some patients with metastatic carcinosarcoma survived for 3–4 years.[9] The prognosis of metastatic carcinosarcoma might differ according to its origin and metastatic site at the time of initial diagnosis. Although irradiation therapy was used to treat our patient, she died 3 years after the tumor was detected. Aggressive therapy, including surgical resection, irradiation therapy and chemotherapy, is required to cure the tumor. Further research is required in order to determine appropriate treatment and evaluate the outcome of this rare type of tumor.

REFERENCES

1 Silverberg SC, Major FJ, Blessing JA. Carcinosarcoma (malignant mixed mesodermal tumor) of the uterus. A gynecologic oncology group pathologic study of 203 cases. *Int J Gynecol Pathol* 1990; **9**: 1–19.

2 Davis PC, Franklin EW. Cancer of the vagina. *South Med J* 1975; **68**: 1239.

3 George E, Manivel JC, Dehner LP, Wick MR. Malignant mixed mullerian tumors. An immunohistochemical study of 47 cases, with hitogenetic considerations and clinical correlation. *Hum Pathol* 1991; **22**: 215–23.

4 Neesham D, Kerdemelidis P, Scurry J. Primary malignant mixed mullerian tumor of the vagina. *Gynecol Oncol* 1998; **70**: 303–7.

5 Peters WA, Kumar NB, Anderses WA, Morley GW. Primary sarcoma of the adult vagina: a clinicopathologic study. *Obstet Gynecol* 1985; **65**: 699–704.

6 Rutledge F. Cancer of the vagina. *Am J Obstet Gynecol* 1967; **97**: 635–49.

7 Wada H, Enomoto T, Fujita M *et al.* Molecular evidence that most but not all carcinosarcomas of the uterus are combination tumors. *Cancer Res* 1997; **57**: 5379–85.

8 Fujii H, Yoshida M, Gong ZX *et al.* Frequent genetic heterogeneity in the clonal evolution of gynecological carcinosarcoma and its influence on phenotypic diversity. *Cancer Res* 2000; **60**: 114–20.

9 Sreenan JJ, Hart WR. Carcinosarcomas of the female genital tract. A pathologic study of 29 metastatic tumor: Further evidence for the dominant role of the epithelial component and the conversion theory of histogenesis. *Am J Surg Pathol* 1995; **19**: 666–74.

10 Peters WA, Kumar NB, Fleming WP. Prognostic features of sarcomas and mixed tumors of the endometrium. *Obstet Gynecol* 1984; **63**: 550–56.

11 Colombi RP. Sarcomatoid carcinomas of the female genital tract (malignant mixed mullerian tumors). *Semin Diagn Pathol* 1993; **10**: 169–75.

Enhancement of osteogenesis on hydroxyapatite surface coated with synthetic peptide (EEEEEEEPRGDT) *in vitro*

D. Itoh,[1] S. Yoneda,[2] S. Kuroda,[2] H. Kondo,[2] A. Umezawa,[3] K. Ohya,[4] T. Ohyama,[1] S. Kasugai[2]
[1]*Removable Prosthodontics, Tokyo Medical and Dental University, 1-5-45, Yushima, Bunkyo-ku, Tokyo, 113-8549, Japan*
[2]*Masticatory Function Control, Tokyo Medical and Dental University, Tokyo, Japan*
[3]*Pathology, Keio University, Tokyo, Japan*
[4]*Department of Phamacology, Hard Tissue Engineering, Tokyo Medical and Dental University, Tokyo, Japan*

Received 5 October 2001; revised 4 February 2002; accepted 7 March 2002

Abstract: Some dental implants are coated with hydroxyapatite (HA), which preferentially binds to bone. Several matrix proteins have an arginine-glycine-aspartic acid (RGD) sequence where cells attach via an integrin receptor. We hypothesized that coating an HA surface with an RGD-containing peptide might enhance the attachment and differentiation of osteoblasts. The HA disks (diameter 34 mm, thickness 1 mm) were treated with a solution (50 mM Tris/HCl and 150 mM NaCl, pH 7.4) containing the peptide EEEEEEEPRGDT, in which the E repetition exerts a high affinity to HA. After washing with phosphate-buffered saline, KUSA/A1 mouse osteoblastic cells were inoculated onto the HA surface and cultured. After 30 min, the number of cells attached to the surface was counted. The DNA content and alkaline phosphatase (ALP) activity were measured after 10 days in culture. Expression of bone matrix proteins was also examined by means of reverse transcriptase–polymerase chain reaction at 7 days; the mineralized area of the culture was also evaluated by staining with Alizarin Red S after 10 days. Treatment with the peptide stimulated cell attachment and increased DNA content and ALP activity. Furthermore, matrix protein expression and mineralized nodule formation were enhanced to a greater extent on the peptide-treated surface than on the nontreated surface. Our results indicate that coating an HA surface with RGD-containing peptide enhances osteoblast attachment and differentiation. This peptide treatment of HA-coated implants may stimulate the osseointegration of the implants. © 2002 Wiley Periodicals, Inc. J Biomed Mater Res 62: 292–298, 2002

Key words: cell attachment; hydroxyapatite; osseointegration; osteoblast; RGD

INTRODUCTION

Hydroxyapatite (HA) is a bioactive material that has chemical direct-bone-bonding capability.[1–4] We previously reported that osteoblastic cells preferentially differentiate on HA and produce bonelike tissue.[5] It is generally accepted that HA enhances bone formation and bone adaptation on its surface. Indeed, HA-coated implants show higher initial integration of osseous tissue than do noncoated titanium implants,[6] and clinical success has been noted,[7,8] especially in low-quality bone such as type 4 bone in the maxilla, with the exception of the mechanical drawbacks of HA-coated implants including resorption, fracture, and fatigue. A 9-year clinical study showed that the survival rate of HA-coated implants placed in the lower jaw after 5 years is over 95%, and especially for implants placed in maxillary type 4 bone, there was a 32.6% failure rate among noncoated titanium implants but a rate of 14.9% in HA-coated implants.[9]

It is accepted that integrin-mediated adhesion of cells to extracellular matrix components is essential for cell migration, proliferation, and differentiation.[10] Bone sialoprotein (BSP), one of the noncollagenous proteins in bone, mediates the attachment of osteoblastic cells[11] and stimulates the differentiation of osteoblasts.[12,13] Bone sialoprotein contains both a consecutive sequence of E (Glu) and an RGD (Arg-Gly-Asp) cell-attachment sequence.[14] The consecutive sequence of E is the likely HA binding site, because synthetic peptides comprising repetitive acidic amino acids (E or D) have a high affinity to HA.[14–17] Interestingly, synthetic peptides consisting of poly-E and RGD sequences (E_7PRGDT) have a high affinity to HA via the poly-E sequence, enhancing the attachment of osteoblastic cells to HA.[18]

Correspondence to: D. Itoh; e-mail: di.rpro@tmd.ac.jp

Recently, several studies showed the effects of biological coatings on cell attachment. It was reported that coating solid surfaces with peptides incorporating both cell-adhesive and heparin-adhesive motifs can enhance the cell-surface interactions including cell attachment.[19] Moreover, a synthetic 15-residue peptide (P-15) with steric similarities to the cell binding site of type I collagen has been reported to promote dermal fibroblast attachment and proliferation.[20]

Based on this body of evidence, we postulated that coating the HA surface with an RGD-containing peptide would enhance both the attachment and the differentiation of osteoblasts. Consequently, osteogenesis would be enhanced on the HA surface. In the current study, we coated HA with the synthetic peptide (E_7PRGDT), inoculated osteoblastic cells onto the surface, and then examined cell attachment, DNA content, and osteoblastic phenotypic expression, including mineralization.

MATERIALS AND METHODS

Preparation of the synthetic peptide

The synthetic peptide E_7PRGDT was synthesized on 4-alkoxylbenzyl resin by the Fmoc synthesis procedure.[21] This peptide contains both the putative HA-binding sequence and the RGD sequence.[18] The peptide was purified by reverse-phase high performance liquid chromatography (HPLC), giving a final product purity of 97.9%.

Preparation of HA disks

Hydroxyapatite disks (nonporous; 1200°C sintered; 34 mm diameter and 1 mm thickness) were kindly provided by Mitsubishi Material Co. (Tokyo, Japan). The surface of the HA disks was polished to eliminate the risk of surface irregularities influencing cell attachment and growth. The analysis of HA surface roughness was performed by atomic force microscopy (AFM, SPI3800 probe station, Seiko Instruments Inc., Chiba, Japan). In AFM analysis, the surface of each HA disk was analyzed at five random locations, each representing an area of 100 × 100 μm. Surface roughness values were expressed as average roughness (Ra). The Ra value varied between 47 and 59 nm, and there were no significant differences in roughness values among the HA disks. The HA disks were washed with Mili-Q water, immersed in acetone, and dry-sterilized for 30 min at 180°C. The sterilized HA disks were placed on a six-well plate (Sumitomo Bakelite Co., Ltd., Tokyo, Japan) with the bottom sealed with 1.0% agar.

The HA disks in the six-well plate were immersed in Tris/HCl solution (50 m*M* Tris/HCl and 150 m*M* NaCl, pH 7.4) containing E_7PRGDT peptides (5, 10, and 20 μg/mL), and the plate was gently shaken at 25°C for 1 h. The HA disks treated with Tris/HCl solution without peptides (noncoated HA) were used as the controls. The HA disks were then washed with phosphate-buffered saline (PBS) and equilibrated with α-MEM (Modified Eagle's Medium; Gibco Laboratories, NY).

Cell culture

Murine KUSA/A1 osteoblastic cells were used in the current study.[22] The cell suspension was seeded into the six-well plates, which were cultured in α-MEM supplemented with 10% fetal bovine serum and 60 μg/mL kanamycin (basal medium), at 37°C in an atmosphere at 95% humidity containing 5% CO_2. After 24 h, the medium was changed to other medium, which was additionally supplemented with 0.2 m*M* phosphate-ester of ascorbic acid (Wako Chemical Co., Osaka, Japan) and 5 m*M* β-glycerophosphate (Sigma Chemical Co., St. Louis, MO). This medium was used in the cultures for the following experiments except cell attachment assay. The medium was changed every 3 days.

Cell attachment assay

The KUSA/A1 cells were inoculated at a density of 8×10^3 cells/cm^2 and cultured on either coated HA (5, 10, and 20 μg/mL) or noncoated HA disks for 30 min. The unattached cells were then collected and the HA disks were rinsed with PBS to collect any remaining unattached cells. The unattached cells were counted using a Coulter Counter (Coulter Electronics Ltd., Luton, Beds, England), and the numbers of attached cells were estimated.

Measurement of DNA content and alkaline phosphatase (ALP) activity

At 10 days, the cells were scraped into 300 μL of the solution (0.1% SDS [sodium dodecylsulfate], 150 m*M* NaCl) and sonicated on ice. The sample was centrifuged and the supernatant recovered. The DNA content was determined by the method of Labarca and Paigen.[23] A portion (50 μL) of the supernatant was mixed with Hoechst 33258 buffer (1 μg/mL Hoechst 33258, 0.05*M* Na_3PO_4, 2.0*M* NaCl, and 2.0 m*M* edetic acid [EDTA], pH 7.4). The fluorescence was read at 356 nm excitation/458 nm emission employing a spectrofluorometer using salmon sperm DNA as the standard. Of the above supernatant, 100 μL was used to test for ALP activity. The ALP activity was measured spectrophotometrically at 405 nm utilizing the ALP B-Test Wako kit (Wako Chemical Co., Japan), which is based on the method of Bessey et al.[24]

RT-PCR

The total RNA of the 7-day culture was extracted using ISOGEN (Nippon Gene Co., Japan), a modified acid gua-

TABLE I
Primers Used and Cycling Conditions in the Current Study

PCR Primer Pair		Melting Temp. (°C)	Annealing Temp. (°C)	Extension Temp. (°C)	Thermal Cycles
OPN	U: 5-CCT CTG AAG AAA CGG ATG ACT-3 D: 5-CTG GGC AAC TCG GAT GAC CTT-3	94	72	55	30
OC	U: 5-ATG AGG ACC CTC TCT CTG CT-3 D: 5-CCG TAG ATG CGT TTG TAG GC-3	94	72	55	30
BSP	U: 5-GTC AAC GGC ACC AGC ACC AA-3 D: 5-GTA GCT GTA TTC GTC CTC AT-3	94	72	55	30
COL I	U: 5-TCT CCA CTC TTC TAG TTC CT-3 D: 5-TTG GGT CAT TTC CAC ATG C-3	94	72	55	25
G3PDH	U: 5-ACC ACA GTC CAT GCC ATC AC-3 D: 5-TCC ACC ACC CTG TTG CTG TA-3	94	72	55	25

nidinium-phenol-chloroform extraction technique.[25] Cells on HA were washed with PBS(−) and scraped before using ISOGEN to prevent extracted RNA from binding to the HA substrata. Cells were homogenized in ISOGEN, and the sample was centrifuged after the addition of chloroform to remove insoluble material. Isopropanol was added to the supernatant and the sample was centrifuged. Total RNA was precipitated and washed with 70% ethanol. After centrifugation, precipitation was dried briefly and dissolved in diethyl pyrocarbonate (DEPC)-treated water. Following the spectrophotometric measurement of the RNA and RNA quality check in agarose gel electrophoresis, total RNA (1 μg) in DEPC aqueous solution was reverse-transcribed to cDNA. The First-Strand cDNA Synthesis Kit (Pharmacia Biotech, United States) consisting of reverse transcriptase and oligo [deoxythymidine (dT)] primer was employed. Primer sequences and the number of thermal cycles required for PCR amplification are presented in Table I. For PCR amplification, initial heating at 94°C for 5 min was followed by the thermal cycle shown in Table I and finally by 72°C for 10 min. The PCR products were subjected to electrophoresis in 2.0% agarose gel and then stained with ethidium bromide, and bands were visualized by ultraviolet transilluminator. The stained gel was analyzed using an imaging densitometer (Bio Rad, GS-670) and a Macintosh computer.

Measurement of mineralized nodule formation

The KUSA/A1 cells were inoculated at a density of 5×10^3 cells/cm^2 and cultured in the experimental medium for 10 days. The cells were then fixed with methanol and stained with Alizarin Red S. Images of the mineralized nodules were acquired employing an imaging densitometer (Bio Rad, GS-670), and analyzed using NIH Image 1.59 software on a Macintosh computer.

Statistical analysis

Data were expressed as mean plus standard deviation for measurement results of cell attachment ratio, DNA content, ALP activity, mineralized area, and expression levels of osteoblastic phenotypes. One-way analysis of variance (ANOVA) with Fisher's protected least significant difference (PLSD) test was used for multiple comparisons to compare with control. The probability level of $p < 0.05$ was regarded as statistically significant.

RESULTS

The KUSA/A1 cells, a murine osteoblastic cell line, attached to the surface of both coated HA and noncoated HA disks. The results of the cell attachment assay are shown in Figure 1. Thirty minutes after cell inoculation, the ratio of cell attachment of KUSA/A1 cells to the noncoated HA was below 40%, whereas it was greater by more than twofold on coated HA. The

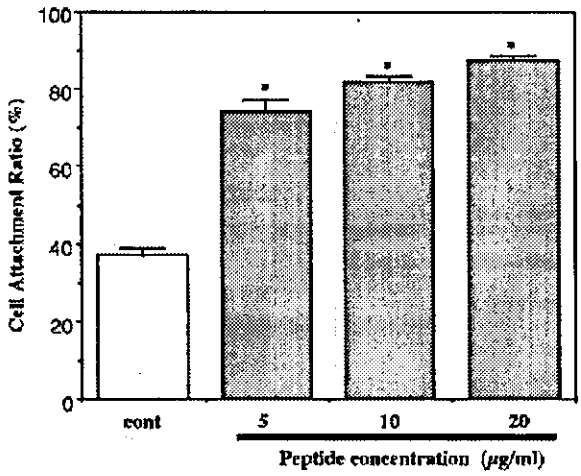

Figure 1. Effect of the E_7PRGDT peptide on osteoblastic cell attachment. The KUSA/A1 cells were inoculated on HA disks coated with the peptide (5–20 μg/mL) for 30 min. The unattached cells were counted by a coulter counter. The ratios of the attached cells to total inoculated cells are presented. Mean + 1 SD (n = 4). *Significantly different from control, $p < 0.05$.

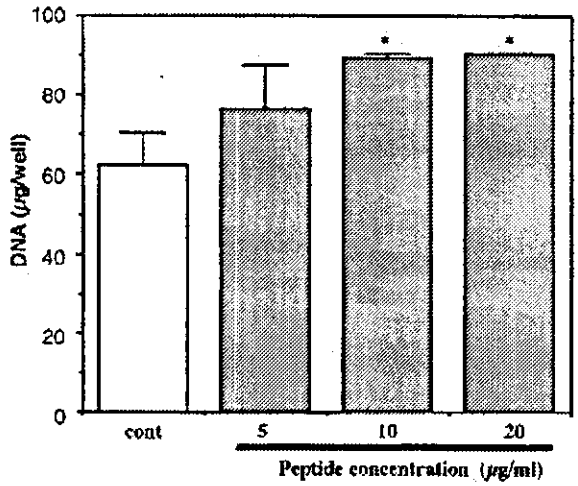

Figure 2. Effect of the E_7PRGDT peptide on DNA content. The KUSA/A1 cells were cultured on HA disks coated with the peptide (5–20 μg/mL). The DNA content was measured at day 10. Mean + 1 SD (n = 4). *Significantly different from control, $p < 0.05$.

ratio of cell attachment of KUSA/A1 cells remarkably increased on coated HA; however, there was no significant difference in attachment by increasing peptide concentration.

As shown in Figure 2, the amount of DNA increased on the coated HA disks and reached a plateau on the disks incubated with 10 μg/mL of the peptide solution. Measurement of ALP activity revealed that ALP activity increased on the disks treated with 10 μg/mL peptide, although ALP activity on the disks treated with 20 μg/mL peptide was similar to the ones on the control disks (Fig. 3).

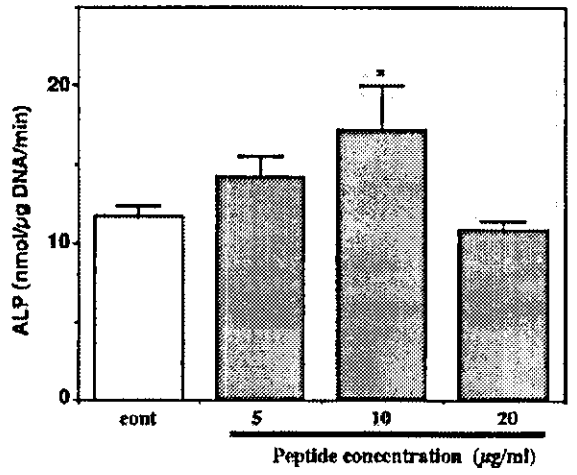

Figure 3. Effect of the E_7PRGDT peptide on ALP activity. The KUSA/A1 cells were cultured on HA disks coated with the peptide (5–20 μg/mL). The ALP activity was spectrophotometrically measured at day 10. Mean + 1 SD (n = 4). *Significantly different from control, $p < 0.05$.

Utilizing RT-PCR, we examined the expression of several genes that are implicated in osteoblastic differentiation, and these results are presented in Figure 4(a,b). Overall, treatment with the E_7PRGDT peptide enhanced the expression of osteopontin (OPN), BSP and osteocalcin (OC), although the expression peaks of these genes was at 5 or 10 μg/mL rather than at the highest concentration of 20 μg/mL. With respect to the expression of type I collagen (COL I), there was no significant difference among the groups.

As shown in Figure 5, the effect of the E_7PRGDT peptide on the mineralized nodule formation was biphasic. Although the peptide enhanced mineralized nodule formation at lower concentrations, its effects declined at higher concentrations. The mineralized

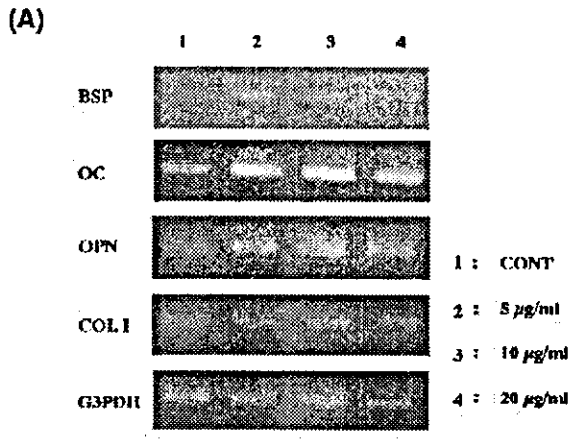

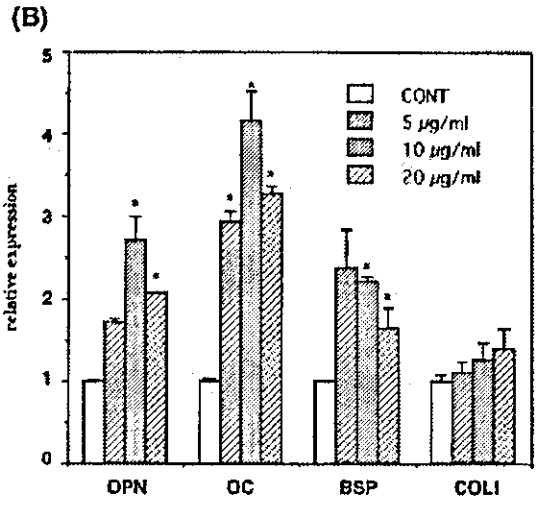

Figure 4. Expression of osteoblastic phenotypes. The KUSA/A1 cells were cultured on HA disks coated with the peptide (5–20 μg/mL). At day 7, after RNA extraction, expression level of osteoblastic phenotypes was examined with RT-PCR. (A) Gel images after ethidium bromide staining. (B) Comparison of mRNA expression levels. Mean + 1 SD (n = 3). *Significantly different from control, $p < 0.05$.

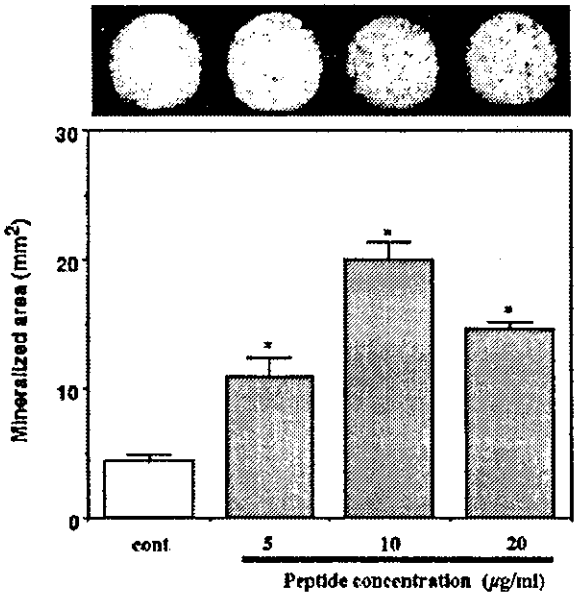

Figure 5. Effect of the E_7PRGDT peptide on mineralized nodule formation in KUSA/A1 cells The KUSA/A1 cells were cultured on HA disks coated with the peptide (5-20 μg/mL). At day 10, the area of mineralized nodule was measured by an image analyzer after staining with Alizarin Red S. Mean + 1 SD (n = 4). *Significantly different from control, $p < 0.05$.

area on every coated HA disk (5, 10, and 20 μg/mL) was greater than that on the noncoated disks.

DISCUSSION

Hydroxyapatite is a bioactive material characterized by its high affinity to components of extracellular matrices and growth factors.[26,27] We also reported that HA has osteoconductive ability that enhances mineralized tissue formation on its surface, strongly suggesting that HA provides an environment favorable to osteoblastic differentiation.[5] Indeed, it is accepted that HA acts well as a dental implant material, providing rapid and tight osseointegration.

The role of noncollagenous proteins in bone has been investigated. Bone sialoprotein is one noncollagenous bone protein, characterized by an RGD cell-attachment sequence and two regions of polyglutamic acid. Bone sialoprotein regulates the attachment of osteoblasts,[10] fibroblasts,[28] and osteoclasts.[29,30] The RGD sequence contributes to cell attachment, whereas polyglutamic acid sequence has a high affinity for HA, which is thought to control HA nucleation. Synthetic peptides[18,31] and recombinant proteins[32-34] have been utilized to investigate the function of BSP in osteoblastic cell attachment and HA nucleation. The E_7PRGDT peptide is such a peptide and has a high affinity to HA.[16,17] When an HA surface is treated with this peptide solution, it is assumed that the E_7PRGDT peptide binds to the HA via the polyglutamic acid sequence and the RGD region of this peptide extrudes in the medium. It was already reported that treating HA with this peptide enhances the attachment of osteoblastic MC3T3-E1 cells to HA.[18] Thus, we postulate that enhancement of osteoblastic cell attachment by this peptide could subsequently affect the growth and differentiation of these cells.

In the current study, we used cells from the KUSA/A1 murine osteoblastic cell line, because KUSA/A1 cells constantly and reproducibly form mineralized nodules within a shorter culture period than required by MC3T3-E1 cells. Similar to previous results seen with MC3T3-E1 cells, the E_7PRGDT peptide treatment enhanced the attachment of KUSA/A1 cells to HA. Conversely, osteoblastic cell attachment to the HA surface is inhibited when the medium contains RGD peptide.[18,35] It is clear that an interaction between the RGD sequence and integrin subunits of osteoblastic cells is crucial for cell attachment to the HA surface to take place.

The E_7PRGDT peptide treatment stimulated the initial cell attachment, and it may also affect subsequent cell attachment after cellular proliferation. Treatment with this peptide increased the DNA amount in the culture at 10 days; however, the degree of growth stimulation triggered by this peptide treatment was less marked than was the stimulation of cell attachment. Thus, treatment of the HA surface with this peptide would appear to provide a favorable situation for cell growth, although the peptide effect is not especially marked.

The ALP activity and expression of the bone matrix proteins, such as OPN, OC, BSP and COL I, are osteoblastic phenotypes, which we examined in the present study. The level of expression of these osteoblastic phenotypes depends on the stage of cellular differentiation. The E_7PRGDT peptide treatment stimulated ALP activity at low concentrations, whereas it did not stimulate ALP activity at the higher concentration of 20 μg/mL. The peptide treatment stimulated the mRNA expression of OPN, OC, and BSP. However, these stimulatory patterns also showed similar tendency: the peak of the expression was at 5 or 10 μg/mL, whereas the expression level declined at 20 μg/mL.

Osteoblastic KUSA A/1 cells produce mineralized nodules, and the E_7PRGDT peptide treatment stimulated mineralized-nodule formation. Clearly, the quantity of mineralized nodules is a cumulative index of the degree of osteoblastic phenotype expression, including ALP activity and matrix production. Thus, it is reasonable that the stimulatory pattern of the peptide treatment to mineralized nodule formation was

similar to the results seen in osteoblastic phenotype expression.

The reason for the decline of osteoblastic phenotype expression and mineralization at 20 μg/mL of the peptide is not clear. For cellular growth and differentiation to take place, adherence to the substrata and development of focal adhesions is essential.[36] However, the cells might have adhered too tightly to the HA surface when HA was treated with an excess amount of the E_7PRGDT peptide. Although excessively tight cellular adhesion to substrata inhibits cellular migration,[37] it is unlikely that this inhibition retards osteoblastic differentiation observed at day 10 in the study, because osteoblasts extensively proliferate and differentiate on the matrices produced by them.

It is not certain how much of the E_7PRGDT peptide attached to the HA surface in the current study. We previously reported that fluorescence-labeled Asp_6 (D_6) peptide preferentially attaches to bone surface after systemic administration to experimental animals and that this peptide remains on bone surface until osteoclasts absorb this bone surface. Thus, the E_7 peptide could also stably attach to the HA surface for a long period. After the E_7PRGDT peptide attached to the HA surface, the RGD part of the peptide might be cleaved in the culture. This RGD fragment could act on the osteoblastic cells by binding to the integrin, consequently inhibiting the differentiation of the cells. However, this is not the main reason for the decline of osteoblastic phenotype expression and mineralization at 20 μg/mL of the peptide, because the amount of the E_7PRGDT peptide was, probably, not enough to exert these effects.

In the current study we demonstrated that E_7PRGDT peptide treatment of HA enhances the attachment of osteoblastic cells and the expression of osteoblastic phenotypes including mineralization, although these stimulation effects are not seen in a simple concentration-dependent manner. The chief advantage of HA as a dental implant material is its high Osseo conductivity. The present results suggest that the E_7PRGDT peptide reinforces the osseoconductivity of HA. When HA is implanted in bone, E_7PRGDT peptide pretreatment modifies the protein absorption on its surface, after which cells that include osteoprogenitors may preferentially attach to its surface, resulting in an increase in osseointegration. However, this is speculation, and further *in vivo* studies are necessary.

The authors are grateful to Dr. R. Fujisawa, Hokkaido University, Japan, for practical advice in conducting the study.

References

1. Gross UM, Muler CM, Voigt C. Comparative morphology of the bone interface with glass-ceramics, hydroxyapatite, and natural coral. In: Davies JE, editor. The bone biomaterial interface. University of Toronto Press; 1991. p 308–320.
2. Neo M, Kotani S, Nakamura T, Yamamuro T, Ohtsuki C, Kokubo T, Bando Y. A comparative study of ultrastructures of the interfaces between four kinds of surface-active ceramic and bone. J Biomed Mater Res 1992;26:1419–1432.
3. Van Blitterswijk CA, Hesseling SC, Grote JJ, Koerten HK, de Groot K. The biocompatibility of hydroxyapatite ceramic: a study of retrieved human middle ear implants. J Biomed Mater Res 1990;24:433–453.
4. Tracy BM, Doremus RH. Direct electron microscopy studies of bone hydroxylapatite interface. J Biomed Mater Res 1984;18: 719–726.
5. Ozawa S, Kasugai S. Evaluation of implant materials (hydroxyapatite, glass-ceramics, titanium) in rat bone marrow stromal cell culture. Biomaterials 1996;17:23–29.
6. Watson CJ, Tinsley D, Ogden AR, Russel JL, Mulay S, Davidson EM. A 3 to 4 year study of single tooth hydroxylapatite coated endosseous implants. Br Dent J 1999;187:90–94.
7. Saadoun AP, LeGall ML. Clinical results and guidelines on Steri-Oss endosseous implants. Int L Periodontol Rest Dent 1992;12:486–495.
8. Meffert RM. Maxilla vs mandible: why use HA? Compendium 1993;(suppl 15): S533–S538; quiz S565–S566.
9. Lozada JL, James RA, Boskovic M. HA-coated implants: warranted or not? Compendium 1993;(suppl 15):S539-S543; quiz S565–S566.
10. Adams JC, Watt FM. Regulation of development and differentiation by the extracellular matrix. Development 1993;117: 1183–1198.
11. Oldberg A, Franzen A, Heinegard D, Pierschbacher M, Ruoslahti E. Identification of a bone sialoprotein receptor in osteosarcoma cells. J Biol Chem 1988;263:19433–19436.
12. Zhou HY, Takita H, Fujisawa R, Mizuno M, Kuboki Y. Stimulation by bone sialoprotein of calcification in osteoblast-like MC3T3-E1 cells. Calcif Tissue Int 1995;56:403–407.
13. Mizuno M, Imai T, Fujisawa R, Tani H, Kuboki Y. Bone sialoprotein (BSP) is a crucial factor for the expression of osteoblastic phenotypes of bone marrow cells cultured on type I collagen matrix. Calcif Tissue Int 2000;66:388–396.
14. Oldberg A, Franzen A, Heinegard D. The primary structure of a cell-binding bone sialoprotein. J Biol Chem 1988;263:19430–19432.
15. Juriaanse AC, Arends J, Ten Bosch JJ. The adsorption of acidic and basic homopolypeptides to whole bovine dental enamel. J Colloid Interface Sci 1980;76:212–226.
16. Fujisawa R, Nodasaka Y, Kuboki Y. Acidic amino acid rich sequences as binding sites of osteonectin to hydroxyapatite crystals. Biochim Biophys Acta 1996;1292:53–60.
17. Kasugai S, Fujisawa R, Waki Y, Miyamoto K, Ohya K. Selective drug delivery system to bone: small peptide (Asp_6) conjugation. J Bone Miner Res 2000;15:936–943.
18. Fujisawa R, Mizuno M, Nodasaki Y, Kuboki Y. Attachment of osteoblastic cells to hydroxyapatite crystals by a synthetic peptide (Glu_7-Pro-Arg-Gly-Asp-Thr) containing two functional sequences of bone sialoprotein. Matrix Biology 1997;16:21–28.
19. Rezania A, Healy KE. Biomimetic peptide surfaces that regulate adhesion, spreading, cytoskeletal organization, and mineralization of the matrix deposited by osteoblast-like cells. Biotechnol Prog 1999;15:19–32.
20. Qian JJ, Bhatnagar RS. Enhanced cell attachment to anorganic bone mineral in the presence of a synthetic peptide related to collagen. J Biomed Mater Res 1996;31:545–554.
21. Austen B. Peptide synthesis. In: Methods in molecular biology, vol. 3. Walker JM, editor. Clifton, NJ: Humana; 1988. p 311–331.
22. Umezawa A, Maruyama T, Segawa K, Shadduck RK, Waheed A, and Hata J. Multipotent marrow stromal cell line is able to induce hematopoiesis in vivo. J Cell Physiol 1992;151:197–205.

23. Labarca C, Paigen K. A simple, rapid, and sensitive DNA assay procedure. Anal Biochem 1987;162:156–159.
24. Bessey OA, Lowry OH, Breck MJ. A method for the rapid determination of alkaline phosphatase with five cubic millimeters of serum. J Biol Chem1946;164:321–326.
25. Chomczynski P, Sacchi N. Single-step method of RNA isolation byacid guanidium thiocyanate-phenol-chloroform extraction. Anal Biochem 1987;162:156–159.
26. Bagambisa FB, Joos U, Schilli W. Interaction of osteogenic cells with hydroxyapatite implant materials in vitro and in vivo. Int J Oral Maxillofac Implants 1990;5:217–226.
27. Hjørting-Hansen E, Worsaase N, Lemons JE. Histologic response after implantation of porous hydroxyapatite ceramic in humans. Int J Oral Maxillofac Implants.1990;5:255–263.
28. Somerman MJ, Fisher LW, Foster RA, Sauk JJ. Human bone sialoprotein I and II enhance fibroblast attachment in vitro. Calcif Tissue Int 1988;43:50–53.
29. EK-Rylander B, Flores M, Wendel M, Heinegard D, Andersson G. Dephosphorylation of osteoclastic tartrate-resistant acid phosphatase. Modulation of osteoclast adhesion in vitro. J Biol Chem 1994;269:14853–14856.
30. Flores ME, Norgard M, Heinegard D, Reinholt FP, Andersson G. RGD-Directed attachment of isolated rat osteoclasts to osteopontin, bone sialoprotein, and fibronectin. Exp Cell Res 1992;201:526–530.
31. Rezania A, Thomas CH, Branger AB, Waters CM, Healy KB. The detachment strength and morphology of bone cells contacting materials modified with a peptide sequence found within bone sialoprotein. J Biomed Mater Res 1997;37:9–19.
32. Harris NL, Rattray KR, Tye CE, Underhill TM, Somerman MJ, D'errico JA, Chambers AF, Hunter GK, Goldberg HA. Functional analysis of bone sialoprotein identification of the hydroxyapatite-nucleating and cell-binding domains by recombinant peptide expression and site-directed mutagenesis. Bone 2000;27:795–802.
33. Stybbs JT III. Generation and use of recombinant human bone sialoprotein and osteopontin for hydroxyapatite studies. Connect Tissue Res 1996;35:393–399.
34. Stybbs JT III, Minz KP, Eanes ED, Torchia DA, Fisher LW. Characterization of native and recombinant bone sialoprotein: delineation of the mineral-binding and cell adhesion domains and structural analysis of the RGD domain. J Bone Miner Res 1997;12:1210–1222.
35. Okamoto K, Matsuura T, Hosokawa R, Akagawa Y. RGD peptides regulate the specific adhesion scheme of osteoblasts to hydroxyapatite but not to titanium. J Dent Res 1998;77:481–487.
36. Burridge K, Fath K, Kelly T, Nuckolls G, Turner C. Focal adhesions: Transmembrane junctions between the extracellular matrix and the cytoskeleton. Ann Rev Cell Biol 1988;4:487–525.
37. Ward MD, Hammer DA. A theoretical analysis for the effect of focal contact formation on cell-substrate attachment strength. Biophys J 1993;64:936–959.

Reprinted from JOURNAL OF MEDICAL GENETICS, December 2002, Vol 39, No 12, p e83

ONLINE MUTATION REPORT

Correlation between a specific Wilms tumour suppressor gene (*WT1*) mutation and the histological findings in Wilms tumour (WT)

R Shibata, A Hashiguchi, J Sakamoto, T Yamada, A Umezawa, J Hata

J Med Genet 2002;**39**:e83[http://www.jmedgenet.com/cgi/content/full/39/12/e83]

Wilms tumour (WT) is the most common malignant neoplasm of the kidney in childhood and accounts for approximately 8% of all childhood solid tumours.[1 2] Fetal rhabdomyomatous nephroblastoma (FRN) is a histological variant of WT characterised by a predominance of rhabdomyogenic components. Clinically, WT of the FRN type presents as a huge mass in younger patients and about 30% of them have bilateral disease. The tumour rarely metastasises or shows aggressive behaviour and it has a good prognosis.[3] The Wilms tumour suppressor gene (*WT1*) on chromosome 11p13 was identified in 1990 and encodes a transcriptional factor containing a domain of four zinc finger motifs.[4 5] Schumacher *et al*[6] reported that a germline mutation in *WT1* predisposes to the development of tumours with stromal predominant histology.[6] We analysed germline and tumour *WT1* in seven cases of WT that were diagnosed as FRN histologically, or contained rhabdomyogenic components, and found the same mutation in five of them.

PATIENTS AND METHODS

Patients

Seven cases of WT who were treated surgically between 1998 and 2001 and contained abundant striated muscle as a stromal component histologically were studied. Cases 3, 4, 5, and 6 also had genitourinary tract malformations (table 1). Cases 3 and 6 were associated with cryptorchidism, case 4 with bilateral cryptorchidism and hypospadias, and case 5 with left ovarian dysgenesis. The tumour was bilateral in every case except case 2. None of the patients showed evidence of renal dysfunction or renal failure. Fresh tumour tissue and peripheral blood samples were obtained from all seven patients. Non-tumorous renal tissue was obtained from case 2. Informed consent was obtained from all patients or their parents.

Key points

- We analysed *WT1* in seven cases of Wilms tumour (WT). The histology of these cases mostly showed FRN or nephroblastic type tumours containing abundant mature rhabdomyomatous components with some immature metanephroblastic tissues.
- In five out of seven cases, we detected the same mutation, which was an ^{1168}C to T substitution in zing finger 3 and resulted in a ^{390}Arg becoming a stop codon (R390X).
- Our results suggest that this specific *WT1* mutation of R390X correlates with this particular histological type of WT showing abundant rhabdomyomatous components.

Histopathological analysis

The resected tumours or biopsy specimens were fixed with 10% formalin and embedded in paraffin. Paraffin sections were stained with haematoxylin and eosin (HE), and histological subtyping of WT was performed according to the classification proposed by the Japanese Society of Pathology. We defined FRN as more than one-third of the tumour mass showing striated muscle differentiation and the nephroblastic type was defined as a tumour which showed triphasic histology containing striated muscle, but its proportion of the tumour was less than one-third.

Abbreviations: WT, Wilms tumour; *WT1*, Wilms tumour suppressor gene; FRN, fetal rhabdomyomatous nephroblastoma; LOH, loss of heterozygosity

Table 1 Clinical and histological features and the results of *WT1* mutations

Case	Age/gender	Clinical description of anormalies	Laterality	Histological subtype	Germline mutations	Tumour mutations
1	11 mth/F	(-)	Bilateral	FRN	(-)	(-)
2	1y /M	(-)	Unilateral	FRN	(-)	1168C→T(R390X) LOH
3	11 mth/M	Cryptorchidism	Bilateral	FRN	1168C→C/T	1168C→T(R390X) Homo
4	9 mth/M	Cryptorchidism, hypospadias	Bilateral	Nephroblastic type striated muscle (+)	1168C→C/T	1168C→T(R390X) Homo
5	7 mth/F	Ovarian dysgenesis	Bilateral	FRN	1168C→C/T	1168C→T(R390X) Homo
6	1 y/M	Cryptorchidism	Bilateral	Nephroblastic type striated muscle (+)	1168C→C/T	1168C→T(R390X) LOH
7	6 mth/F	(-)	Bilateral	Nephroblastic type striated muscle (+)	(-)	(-)

Table 2 PCR and sequence primers

	PCR		Sequence	
Exon	Name	Sequence	Name	Sequence
1	WT256	AGCCAGAGCAGCAGGGAGTC	SEQ1-S	GGCATCTGGGCCAAGTTAGG
	WTEX1R2	CGGTCAAAAGGGGTAGGAGA	SEQ1-A	CCTAGAGCGGAGAGTCCCTG
2	2B-S	TGGCTGGTTCAGACCCACTG	SEQ2-S	TGCCCCGTCTTGCGAGAGCA
	2B-A	AGAGGAGGATAGCACGGAAG	SEQ2-A	GCACGGAAGAAGGGGAGAAG
3	3B-S	CCAGGCTCAGGATCTCGTGT	SEQ3-S	ATCTCGTGTCTCCCCCAACC
	3B-A	GGCGTCTCGTGCCTCCAAGA	SEQ3-A	GTGCCTCCAACACCCTGCAT
4	4B-S	TGTGGAGGCTTGCACTTTCA	SEQ4-S	GAAGAAACAGTTGTGTATTATTTTG
	4B-A	GCCCTTTCTTCTAAAACTGT	SEQ4-A	ATGGTTCAAACAGGTATAAGTTACT
5	5B-S	TCACTGGATTCTGGGATCTG	SEQ5-S	CTGGGATCTGGGGGGCTTGCCA
	5B-A	AGTCCTAACTCCTGCATTGC	SEQ5-A	CCCCAGGTGCCAGTCAGCAAGG
6	6B-S	AAAACCATCATTCCCTCCTG	SEQ6-S	TTTCCAAATGGCGACTGTGAGC
	6B-A	CAAAGAGTCCATCAGTAAGG	SEQ6-A	GGTAAGTAGGAAGAGGCAGTGC
7	7F-S	GTGCTCACTCTCCCTCAAGA	SEQ7-S	TCCCTCAAGACCTACGTGAATGTTC
	7F-A	GTGAGAGCCTGGAAAAGGAGC	SEQ7-A	TTGAACCATGTTTGCCCAAGACTGG
8	8-S	AGATCCCCTTTTCCAGTATC	SEQ8-S	AGATCCCCTTTTCCAGTATC
	8C'-A	CAACAACAAAGAGAATCA	SEQ8-A	AAATCAACCCTAGCCCAAGG
9	9C-S	AAGTCAGCCTTGTGGGCCTC	SEQ9-S	CCCACATTGGTTAGGGCCGAGGCTA
	9C-A	TTTCCAATCCCCTCTCATCAC	SEQ9-A	TAGGGCCGAGGCTAGACCTTCTCT
10	10C-S	CACTCGGGCCTTGATAGTTG	SEQ10-S	TTTCCAATCCCCTCTCATCAC
	10C-A	GTCAGACTTGAAAGCAGTTC	SEQ10-A	TGTGCCTGTCTCTTTGTTGC

DNA preparation

Mononuclear cells were isolated from the patients' peripheral blood. Tumour tissue and non-tumorous renal tissue were stored at −80°C until used. DNA was extracted from leucocytes and tumour tissue by the SDS-proteinase K method with slight modifications, as described previously.[7] Amplification of exons 1 to 10 was performed by PCR. Direct sequencing of the PCR products was performed with a MegaBACE 1000 DNA Sequencing System (Amersham Biosciences, Florida, USA). The precise methods have been described previously.[8] The PCR and sequence primers used are shown in table 2.

Polymorphic analysis of *WT1*

We used a polymorphic marker, WT1-P, to investigate whether the mutation detected in *WT1* in the tumour cells was homozygous or hemizygous as a result of loss of heterozygosity (LOH). This marker detects a GT polymorphism in the 3' non-coding region of exon 10 of *WT1*.[9] We used primers WT1P2-1

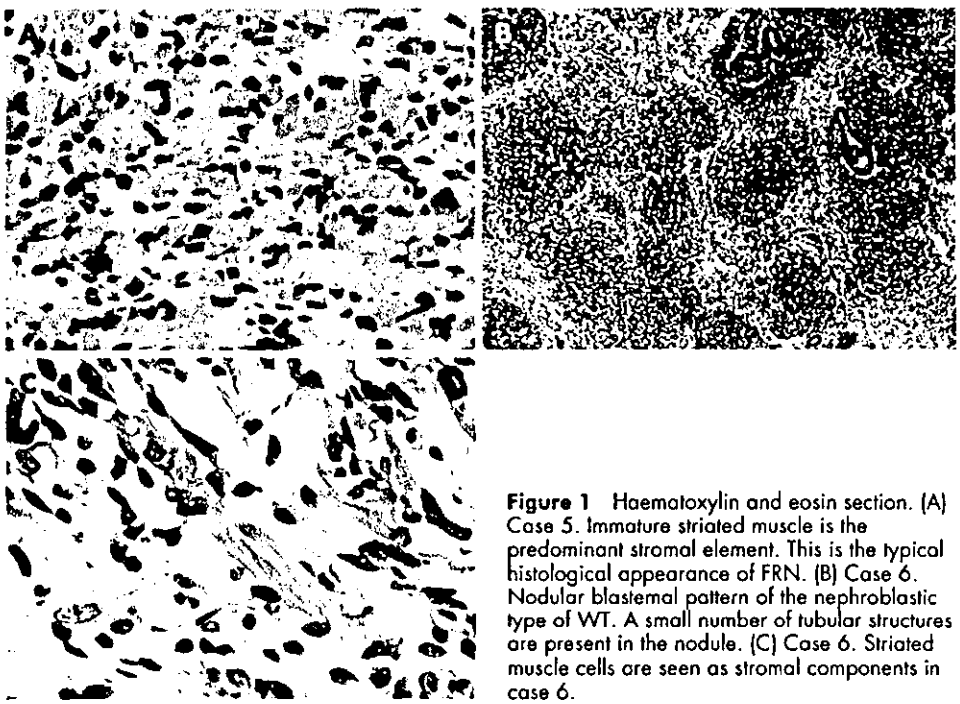

Figure 1 Haematoxylin and eosin section. (A) Case 5. Immature striated muscle is the predominant stromal element. This is the typical histological appearance of FRN. (B) Case 6. Nodular blastemal pattern of the nephroblastic type of WT. A small number of tubular structures are present in the nodule. (C) Case 6. Striated muscle cells are seen as stromal components in case 6.

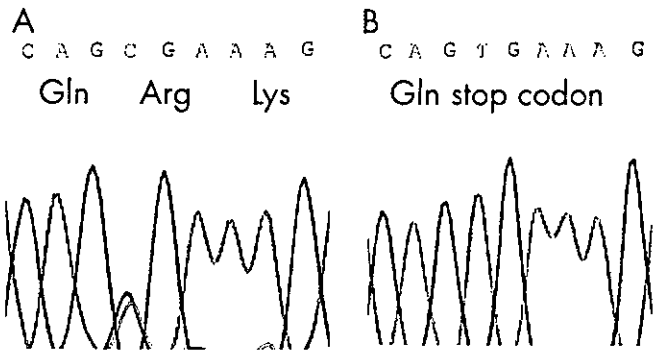

Figure 2 Results of DNA sequence analyses of germline (A) and tumour samples (B) with a *WT1* mutation. (A) A heterozygous point mutation, 1168C/T, was found in exon 9 in the germline of the patient and her father. (B) A point mutation, 1168C/T, changes the codon for ^{390}Arg into a stop codon in the tumours.

(5′-CTTACTGGGTGAGGAAATCC-3′) and WT1P2-2 (5′-ACAGTAATTTCAAGCAACGG-3′) and an ALF win Fragment Analyzer (Amersham Biosciences). All procedures were approved by the Ethical Committee of the Keio University School of Medicine.

RESULTS

The clinical and pathological features and the results of the *WT1* mutations are summarised in table 1. All seven patients were under 1 year of age. Cases 3, 4, 5, and 6 were complicated by congenital genitourinary malformations. The WT was bilateral in every case except case 2. Cases 1, 2, 3, and 5 showed the typical histological features of FRN (fig 1A). Cases 4, 6, and 7 were the nephroblastic type (fig 1B) and contained striated muscle components (fig 1C).

DNA sequence analyses indicated the same constitutional point mutations in exon 9 in cases 3, 4, 5, and 6. The mutation was a 1168C-T substitution in zinc finger 3 and resulted in a ^{390}Arg becoming a stop codon (R390X). There was a heterozygous mutation in the same codon in the germline of cases 3, 4, 5, and 6 (fig 2). Case 2 showed mutation R390X in the tumour, but no mutations were found in the germline. No *WT1* mutations were detected in cases 1 or 7.

The results of the polymorphic analysis of 11p13 are also summarised table 1. The germline in case 5 contained 124 bp and 132 bp bands at WT1-P. These bands were also detected in the bilateral tumours (fig 3A), and we concluded that the *WT1* mutation in the tumours were heterozygous. Cases 3 and 4 also showed heterozygous mutations in tumour tissue (data not shown). DNA isolated from mononuclear cells and the non-tumorous renal tissue of case 2 contained 124 bp and 130 bp bands at WT1-P. The tumour showed only a 124 bp band and it was concluded to show LOH (fig 3B). Case 6 also showed LOH in tumour tissue at WT1-P (data not shown).

DISCUSSION

We found the same mutation of *WT1* in five of the seven cases of WT that were classified as FRN histologically or contained abundant rhabdomyogenic components. Our findings suggested that this specific *WT1* mutation, R390X, is correlated with the histological features of WT.

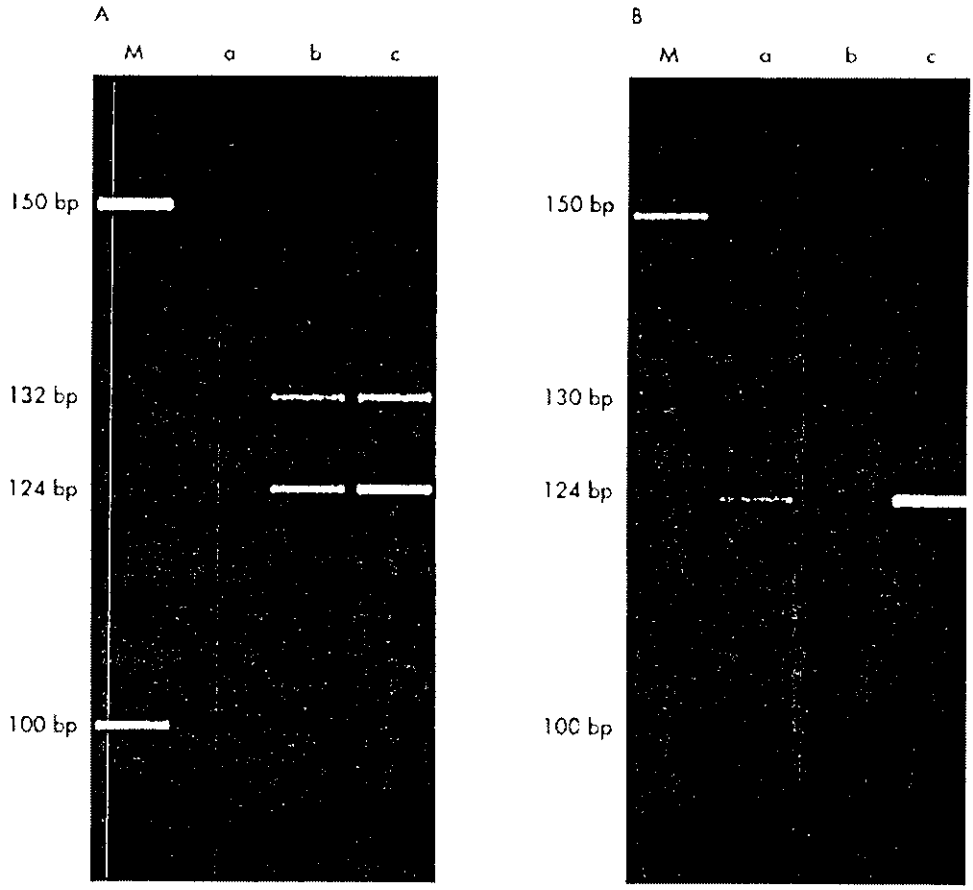

Figure 3 Polymorphic analysis of *WT1*, detecting a GT polymorphism in the 3′ non-coding region of exon 10. M, external markers of 100 bp and 150 bp. (A) Case 5. (a) Germline of the patient; (b) left tumour sample; (c) right tumour sample. A 124 bp and 132 bp band were identified in the germline cells (a) and the both tumour samples (b and c). Lanes a, b, and c show 100 bp and 150 bp bands as internal markers. (B). Case 2. (a) Germline of the patient; (b) non-tumorous renal tissue; (c) tumour sample. A 124 bp and 130 bp band were identified in the germline cells (a) and the non-tumorous renal tissue (b). However, only the 124 bp band was detected in the tumour sample (c). Lanes a, b, and c show 100 bp and 150 bp bands as internal markers.

Cases 3, 4, 5, and 6 were found to have the same constitutional point mutations, a change from 1168C to T in zinc finger 3, resulting in ^{390}Arg becoming a stop codon. Case 2 had the R390X mutation in the tumour. During translation, this nonsense mutation leads to protein truncation, and the result is that the last zinc finger necessary for DNA binding of *WT1* is missing. Interrupted DNA binding to the target genes of *WT1* with loss of the last zinc finger has previously been shown by electrophoretic mobility shift assays.[10] Loss of *WT1* function has been reported to be the underlying cause of tumour development. Miyagawa *et al*[11] reported that loss of *WT1* function leads to ectopic myogenesis in WT and suggested that normal expression of WT1 might prevent the metanephric-mesenchymal stem cells of the kidney from differentiating into skeletal muscle.[11] Three of the five cases that had the *WT1* mutations, cases 2, 3, and 5, were classified as FRN. Cases 4 and 6 were the nephroblastic type and contained striated muscle as stromal components. It could not be concluded that all WTs with the R390X mutation are FRN histologically, but the results at least suggested a correlation between this mutation and rhabdomyomatous histology of WT.

In earlier studies, mutation R390X had been found in patients with sporadic unilateral WT, in a patient with bilateral WT, and in a patient with WT associated with urogenital malformation.[12–14] This mutation has also been detected in a patient with acute promyelocytic leukaemia[15] and a patient with an isolated genital malformation without WT.[16] However, the histological findings in the WTs with the R390X mutation have not been published previously. Histological information in these cases would show whether our hypothesis is more likely or not.

Schumacher *et al*[6] reported that a germline mutation in *WT1* predisposes to the development of tumours with predominantly stromal histology.[6] Case 2 had no germline mutation; however, since Nakadate *et al*[17] reported that not only germinal *WT1* mutation/deletion but somatic *WT1* deletion/mutation correlated with the predominantly stromal histology,[17] the somatic mutation appears to be associated with the histology in case 2.

Some authors have reported *WT1* mutations in WT patients with congenital genitourinary malformations in the absence of renal disorders.[6 18–20] Huff *et al*[21] hypothesised that the truncated protein resulting from *WT1* mutation is non-functional and causes genitourinary malformation by a dose effect of decreasing normal WT1 protein. Cases 3, 4, 5, and 6, which had *WT1* mutations, exhibited congenital genitourinary malformations, suggesting that the loss of WT1 function may cause genitourinary malformation.

Bilateral WT is explained by the two hit inactivation mechanism of a tumour suppressor gene, as proposed by Knudson and Strong.[6 22 23] Cases 3, 4, 5, and 6 presented with bilateral disease, and a heterozygous mutation was detected in their germline and either LOH (case 6) or a homozygous mutation (cases 3, 4, and 5) was found in their tumour specimens. These findings support the two hit inactivation model in bilateral WT. Based on the results of this study, the loss of WT1 expression caused by the R390X mutation appears to be related to the histological findings, genitourinary malformations, and tumorigenesis, at least in bilateral WT. The tumours in cases 1 and 7 contained rhabdomyomatous components and had bilateral disease, but no *WT1* mutation was detected in them. They had no evidence of congenital genitourinary malformations. Another mechanism may be related to the tumorigenesis of bilateral WT without congenital genitourinary malformations.

CONCLUSION

We found that a specific *WT1* mutation of R390X correlates with the histology of WT. WTs with this mutation tend to be FRN or to contain rhabdomyogenic components histologically. This mutation appears to be strongly correlated with not only the histological features but with tumorigenesis in bilateral WTs with congenital genitourinary malformations. However, this report is on only seven cases and we need to investigate more cases of unilateral FRN or cases with FRN but no congenital abnormalities to see if they show *WT1* mutation or not.

ACKNOWLEDGEMENTS

We thank Drs Y Tanaka (Kanagawa Children's Medical Centre), Y Nakatani and Y Inayama (Hospital of Yokohama City University), K Hashizume and Y Kanamori (University of Tokyo Faculty of Medicine), J Miyauchi and Y Tsunematsu (National Centre for Child Health and Development), Y Hayashi (Tohoku University School of Medicine), H Shima and N Konishi (Hyogo College of Medicine), and Y Ogawa (Saitama Children's Medical Centre) for providing samples and clinical data. We thank Miss Y Nakamura for her technical assistance. This work was supported by a Grant-in-Aid for Scientific Research from the Ministry of Education, Culture, Sports, Science, and Technology (11557021, 13470053, 13022264 and 11167274), as well as Cancer Research Grants from the Ministry of Health, Labour and Welfare (9-14, 10D-1).

Authors' affiliations

R Shibata, A Hashiguchi, T Yamada, A Umezawa, J Hata, Department of Pathology, Keio University School of Medicine, Tokyo, Japan
J Sakamoto, Department of Paediatric Surgery, University of Tokyo Faculty of Medicine, Tokyo, Japan
J Hata, National Research Institute for Child Health and Development, Tokyo, Japan

Correspondence to: Dr J Hata, National Research Institute for Child Health and Development, 3-35-31 Taishido Setagaya-ku, Tokyo 154-8567, Japan; jhata@nch.go.jp

REFERENCES

1 **Coppes MJ**, Pritchard-Jones K. Principles of Wilms' tumor biology. *Urol Clin North Am* 2000;**27**:423-33.
2 **Lee SB**, Haber DA. Wilms tumor and the WT1 gene. *Exp Cell Res* 2001;**264**:74-99.
3 **Wigger HJ**. Fetal rhabdomyomatous nephroblastoma-a variant of Wilms' tumor. *Hum Pathol* 1976;**7**:613-23.
4 **Call KM**, Glaser T, Ito CY, Buckler AJ, Pelletier J, Haber DA, Rose AE, Kral A, Yeger H, Lewis WH, Jones C, Housman DE. Isolation and characterization of a zinc finger polypeptide gene at the human chromosome 11 Wilms' tumor locus. *Cell* 1990;**60**:509-20.
5 **Gessler M**, Pouska A, Cavenee W, Neve RL, Orkin SH, Bruns GAP. Homozygous deletion in Wilms tumours of a zinc-finger gene identified by chromosome jumping. *Nature* 1990;**343**:774-8.
6 **Schumacher V**, Schneider S, Figge A, Wildhardt G, Harms H, Schmidt D, Weirich A, Ludwig R, Royer-Pokora B. Correlation of germ-line mutations and two-hit inactivation of the WT1 gene with Wilms tumors of stromal-predominant histology. *Proc Natl Acad Sci USA* 1997;**94**:3972-7.
7 **Kikuchi H**, Akasaka Y, Kurosawa Y, Yoneyama H, Kato S, Hata J. A critical mutation in both WT1 alleles is not sufficient to cause Wilms' tumor. *FEBS Lett* 1995;**360**:26-8.
8 **Takata A**, Kikuchi H, Fukuzawa R, Ito S, Honda M, Hata J. Constitutional *WT1* correlates with clinical features in children with progressive nephropathy. *J Med Genet* 2000;**37**:698-701.
9 **Tadokoro K**, Oki N, Sakai A, Fujii H, Ohshima A, Nagafuchi S, Inoue T, Yamada M. PCR detection of 9 polymorphisms in the WT1 gene. *Hum Mol Genet* 1993;**2**:2205-6.
10 **Little M**, Holmes G, Bickmore W, Heyningen V, Hastie N, Wainwright B. DNA binding capacity of the WT1 protein is abolished by Denys-Drash syndrome WT1 point mutations. *Hum Mol Genet* 1995;**4**:351-8.
11 **Miyagawa K**, Kent J, Moore A, Charlieu JP, Little MH, Williamson KA, Kelsey A, Brown KW, Hassam S, Briner J, Hayashi Y, Hirai H, Yazaki Y, Heyningen V, Hastie ND. Loss of WT1 function leads to ectopic myogenesis in Wilms' tumour. *Nat Genet* 1998;**18**:15-7.
12 **Little MH**, Prosser J, Condie A, Smith PJ, Heyningen V, Hastie ND. Zinc finger point mutations within the WT1 gene in Wilms tumor patients. *Proc Natl Acad Sci USA* 1992;**89**:4791-5.
13 **Gessler M**, Konig A, Arden K, Grundy P, Orkin S, Sallan S, Peters C, Ruyle S, Mandell J, Li F, Cavenee W, Bruns G. Infrequent mutation of the WT1 gene in 77 Wilms' tumors. *Hum Mutat* 1994;**3**:212-22.
14 **Little M**, Wells C. A clinical overview of WT1 gene mutations. *Hum Mutat* 1997;**9**:209-25.
15 **King-Underwood L**, Renshaw J, Pritchard-Jones K. Mutations in the Wilms' tumor gene WT1 in leukemias. *Blood* 1996;**87**:2171-9.
16 **Kohler B**, Schumacher V, l'Allemand D, Royer-Pokora B, Grutters A. Germline Wilms tumor suppressor gene (WT1) mutation leading to isolated genital malformation without Wilms tumor or nephropathy. *J Pediatr* 2001;**138**:421-4.
17 **Nakadate H**, Yokomori K, Watanabe N, Tsuchiya T, Namiki T, Kobayashi H, Suita S, Tsunematsu Y, Horikoshi Y, Hatae Y, Endo M,

Kodama Y, Eguchi H, Toyoda Y, Kikuta A, Kobayashi R, Kaneko Y. Mutations/deletions of the WT1 gene, loss of heterozygosity on chromosome arms 11p and 11q, chromosome ploidy and histology in Wilms' tumors in Japan. *Int J Cancer* 2001;**94**:396-400.

18 **Pelletier J**, Bruening W, Li FP, Haber DA, Glaser T, Housman DE. WT1 mutations contribute to abnormal genital system development and hereditary Wilms' tumour. *Nature* 1991;**353**:431-4.

19 **Kohler B**, Schumacher V, Schulte-Overberg U, Biewald W, Lennert T, l'Allemand D, Royer-Pokora B, Gruters A. Bilateral Wilms tumor in a boy with severe hypospadias and cryptorchidism due to a heterozygous mutation in the WT1 gene. *Pediatr Res* 1999;**45**:187-90.

20 **Sakamoto J**, Takata A, Fukuzawa R, Kikuchi H, Sugiyama M, Kanamori Y, Hashizume K, Hata J. A novel wt1 gene mutation associated with Wilms' tumor and congenital male genitourinary malformation. *Pediatr Res* 2001;**50**:337-44.

21 **Huff V**. Genotype/phenotype correlations in Wilms' tumor. *Med Pediatr Oncol* 1996;**27**:408-14.

22 **Knudson AG Jr**, Strong LC. Mutation and cancer: a model for Wilms' tumor of the kidney. *J Natl Cancer Inst* 1972;**48**:313-24.

23 **Huff V**, Miwa H, Haber DA, Call KM, Housman D, Strong LC, Saunders GF. Evidence for WT1 as a Wilms tumor (WT) gene: intragenic germinal deletion in bilateral WT. *Am J Hum Genet* 1991;**48**:997-1003.

CLINICO-PATHOLOGICAL CONFERENCE

A case of dilated cardiomyopathy with end-stage heart failure treated by prolonged continuous hemodiafiltration

Satoshi Ogawa, Shin-ichiro Matsumura, Tsutomu Yoshikawa, Toru Satoh, Hiroo Kumagai, Hideo Mitamura,[1] Shiro Iwanaga[2] and Akihiro Umezawa[3]

Departments of Internal Medicine, [1]The Suntory Fund for Advanced Cardiac Therapeutics, [2]Laboratory Medicine, [3]Pathology, School of Medicine, Keio University, Tokyo, Japan

(Received for publication on February 27, 2002)

Abstract. A 55-year-old Asian man first visited to our hospital with complaining of exertional dyspnea eight years ago, and was diagnosed as having idiopathic dilated cardiomyopathy. One of his siblings also suffered from idiopathic dilated cardiomyopathy. His symptoms became worse gradually, and he was hospitalized again because of disturbance of consciousness on February 21, 2001. Hemodynamic monitoring with a Swan-Ganz catheter was started, which revealed that the cardiac index was 1.1 L/min/BSA, cardiac output 1.8 L/min, and pulmonary artery pressure 43/33 mmHg. The echocardiographic observation showed that the left ventricular ejection fraction was 32%, and serum BNP was elevated to 5,411 pg/mL. Multi-organ failure including renal and hepatic dysfunction developed because of the low cardiac output status. Continuous hemodiafiltration (CHDF) was introduced to reduce the volume overload, improve renal failure, and eliminate adverse cytokines. Although his hemodynamic status was temporarily improved after starting CHDF, weaning from CHDF was difficult and he finally died from cardiogenic shock after two month of intensive therapy. The autopsy showed thinning of the left ventricular wall, and histological examination revealed diffuse fibrous hyperplasia and myocardial fiber deficit in the ventricular myocardium. CHDF was effective in reducing the volume overload and improving renal function; however, heart transplantation is inevitable for the patients with severe heart failure due to dilated cardiomyopathy. (Keio J Med 51 (3): 165–177, September 2002)

Key words: dilated cardiomyopathy, continuous hemodiafiltration, autopsy, heart failure, unconsciousness

Dr. Ogawa (Moderator): I declare the 1042nd clinico-pathological conference (CPC) open. The case for discussion in today's CPC is a patient who died from gradual worsening of his cardiac function over a course of approximately 8 years. The physician-in-charge, Dr. Matsumura, will first describe the clinical course of this patient.

Dr. Matsumura (Internal Medicine): The patient presented complaining of exertion-related dyspnea on climbing stairs or walking up a slope since March 1993. He visited the Cardiopulmonary Division at our hospital in April 1993. After he was admitted to the hospital, cardiac catheterization and left ventriculography were performed, and revealed contractile dysfunction of the left ventricle, which was manifested by diffuse hypokinase and a reduced ejection fraction (EF, 11%). A myocardial biopsy further revealed hypertrophy of myocardial cells and interstitial fibrosis. There was no evident infectious, metabolic, systemic, or hereditary etiology. The patient was diagnosed as having dilated cardiomyopathy (DCM). Treatment with an anticoagulant (Warfarin®), digitalis glycoside, an angiotensin-converting enzyme (ACE) inhibitor, and furosemide was started. The patient was then discharged from the hospital and treatment was continued on an outpatient basis.

In the months of June and October of 1997, the patient developed acute exaggeration of his heart failure, precipitated by a common cold, and he was admitted to our hospital. Oral administration of pimobendan was

This is a record of the 1042nd CPC of Keio University Hospital, held on January 30, 2002.
Reprint requests to Dr. Satoshi Ogawa, Department of Internal Medicine, School of Medicine, Keio University, 35 Shinanomachi, Shinjuku-ku, Tokyo 160-8582, Japan

started on October. From October 1998, his dyspnea on exertion (DOE) became progressively worse, and in April 2000, he developed the symptom of chest oppression at night. Holter ambulatory ECG recording performed in January 1999 revealed non-sustained ventricular tachycardia (max. 11 beats in a run). At 5:00 a.m. on February 21, 2001, his wife, who was sleeping beside him, noticed that he was breathing hard. He did not respond to her calls, and she immediately called for an ambulance. He was taken to Nihon University Surugadai Hospital. On initial examination, dyspnea and cyanosis were observed. His consciousness level was slightly below normal, and systolic blood pressure was about 70 mmHg. Following endotracheal intubation, artificial ventilation, and intravenous infusion of dobutamine and furosemide, the patient's consciousness improved rapidly. He was transferred to our hospital on February 27.

Dr. Ogawa: So, the clinical course of the patient's illness was as follows: The patient first presented with the clinical features of heart failure in 1993, and he was clinically diagnosed as having DCM. Despite intensive therapy, however, the heart failure became worse gradually and progressively. At one point, he was admitted with loss of consciousness to another hospital. Thereafter, he was again admitted to our Keio University Hospital for thorough examination and treatment.

Echocardiography performed in 1994 revealed end-diastolic and end-systolic left ventricular diameters of 5.9 cm and 4.4 cm, respectively, and cardiac pool scintigraphy (MUGA) revealed a left ventricular EF of about 40%. These dimensions improved slightly to 5.2 cm and 4.2 cm, respectively, in the year 1996, but they increased again in 1998 and 1999; in particular, the end-systolic diameter increased to 5.2 cm, indicating that the contractile function of the left ventricle had decreased considerably.

The patient first presented with dyspnea on exertion in March 1993. Are there data from earlier medical examinations?

Dr. Matsumura: There is one earlier mention of right axis deviation on ECG; however, no other ECG changes were recorded. The patient was apparently in good health in 1982, when he was involved in a traffic accident in the State of Kuwait and underwent surgery on his right lung. Subsequently, he developed slight dyspnea on exertion. The symptom worsened rapidly in 1993, and he was referred to our hospital.

Dr. Ogawa: As for the 11 beat run of non-sustained ventricular tachycardia revealed by the Holter ECG in 1999, was his morbid condition relatively stable during the period when the tachycardia was observed? Or was the non-sustained ventricular tachycardia associated with worsening of his heart failure?

Dr. Matsumura: In 1993, his symptoms of heart failure were relatively mild, classified as New York Heart Association (NYHA) functional class II. A little later, he presented with worsening of the heart failure due to a common cold, and he was admitted to our hospital. On admission, the NYHA functional class found to have worsened from Class II to Class III. When this improved again to Class II (IIM), he was discharged from our hospital. The symptoms thereafter gradually worsened again, and runs of non-sustained ventricular tachycardia were observed on the Holter ECG recording associated with worsening of the heart failure.

Dr. Ogawa: Was the treatment of the tachycardia detected by Holter ECG undertaken on an outpatient basis?

Dr. Matsumura: Yes, it was.

Dr. Ogawa: If so, can we understand that the Holter monitoring was not performed specifically during the period when his heart failure had become worse?

Dr. Matsumura: Yes, we can. Holter ECG monitoring was performed routinely and was not related to the worsening of his heart failure.

Dr. Ogawa: We can therefore say that the non-sustained ventricular tachycardia was incidentally detected.

The patient's chief compliant seems to have been consciousness disturbance; when his wife, who was lying beside him in bed, called out to him at 5:00 a.m. in the morning, she noticed that he did not respond. Is that right?

Dr. Matsumura: Yes, it is.

Dr. Ogawa: I wonder if the ambulance personnel detected any abnormalities in his vital signs that could be responsible for the consciousness disturbance on that occasion? Is there any record?

Dr. Matsumura: His consciousness level was slightly below normal, but it was apparently returning to normal when he was taken into the ambulance. The ECG recorded then also did not show any ventricular tachycardia or ventricular fibrillation. The possibility of low cardiac output due to DCM, or transient arrhythmias, such as spontaneously converted ventricular tachycardia that terminated spontaneously having caused the syncope, cannot, however, be ruled out.

Dr. Ogawa: How was the control of his coagulation parameters with the dose of Warfarin® during this period? Was he taking an appropriate dose of Warfarin®?

Dr. Matsumura: The thrombotest was supported to 10–20%, which suggests favorable control by the Warfarin®. Nor did echocardiography show any evidence of intracardiac thrombus during his course. This echocardiographic finding, together with the appropriate control by Warfarin®, indicate that it is unlikely that cerebral embolism may have been responsible for this syncopal episode. A brain CT was not conducted because the patient was in poor general condition.

Table 1 Vital Signs and Acute Clinical Settings

	Consciousness	Breathing	Pulsation
Normal	+	+	+
Peripheral Artery Occlusion	+	+	−
Coma	−	+	+
Apnea	−	−	+
Choke	±	−	+
Shock	±	+	±
Cardiac Arrest	−	−	−

Dr. Ogawa: What do you think of this case, Dr. Mitamura?

Dr. Mitamura (The Suntory Fund for Advanced Cardiac Therapeutics): I would like to make a few points. As for the labored breathing and absence of response to verbal commands, I doubt whether we can refer to the patient's state here as "syncope". When we use the term "syncope", it usually refers to a condition of complete muscular weakness associated with unconsciousness; labored breathing therefore is not characteristic of syncope. Syncope in this sense generally results from a transient and steep fall of blood pressure. It is also important to know how long the labored breathing was sustained in the patient. To sum up, rather than suffering from an episode of "syncope," this patient was probably taken to the hospital in a so-called state of shock with sustained moderate hypotension, or the main cause of the patient's condition may have been dysfunction of the central nervous system (Table 1).

The following possibilities should be considered in this circumstance, other than DCM: (1) The possibility of ventricular tachycardia having spontaneously terminated when the patient was taken to the hospital should be considered as the most likely; (2) and, despite the favorable control of warfarinization, there is still the possibility of cerebral infarction having occurred due to a cerebral embolism derived from an intraventricular thrombus because of poor left ventricular function; (3) there is also the probability of cerebral hemorrhage having occurred due to an excess dose of Warfarin®; (4) the possibility of hemorrhagic shock having been caused by gastrointestinal hemorrhage or hemorrhage from other sites; and (5) the possibility of pulmonary embolism, in which condition the blood pressure of patients with very poor cardiac function who are bedridden over a long period of time, suddenly declines.

Dr. Ogawa: Thank you very much. How about his family history?

Dr. Matsumura: The patient's younger brother was diagnosed as having DCM at the age of 45 years.

Dr. Tsuji (5th-year medical student): Could the history of pulmonary contusion on the right side in 1982 be related to the slight decrease in respiratory sound on the right side?

Dr. Matsumura: As is evident from the chest X-rays, the patient had developed thoracic deformity and collapse of the right lung consequent to the pulmonary contusion. This is probably the cause for the muted respiratory sound on the right side.

Dr. Ogawa: What was the nature of this pulmonary injury? Could you explain it in greater detail?

Dr. Matsumura: When he was driving, his car collided head-on with another car. At that time, two other people who were in the car with him died instantly, so the accident was apparently a major traffic accident.

Dr. Ogawa: I wonder how we can correlate his morbid condition, DCM, with the accident. For instance, it has been reported that myocardial injury of the right ventricle or tricuspid regurgitation can occur following steering wheel injury. The patient, however, had not been detected as having any significant physical abnormalities in medical check-ups undertaken subsequent to the accident. Am I right?

Dr. Matsumura: Yes, that's right.

Dr. Ogawa: There is no history to suggest that the patient was a habitual drinker. The presence of a drinking history is very important in making a differential diagnosis. Now, will you please describe the patient's clinical condition on admission to our hospital?

Dr. Matsumura: The blood pressure was 110/80 mmHg, and the pulse was 100 beats per minute. The respiratory rate was 26 per minute. He was fully conscious. The external jugular vein was distended. In regard to the heart sounds, P2 was loud, and 3rd and 4th heart sounds were audible. A systolic murmur could be heard between the cardiac apex and the 4th intercostal space at the left margin of the sternum. Breath sounds were decreased on the right side of the chest, and there were no added sounds. The liver was palpable by 3 QFB and there was some tenderness below the right costal margin. There was no pretibial edema.

Laboratory examination revealed normocytic normochromic anemia and increase in the serum levels of fibrinogen and fibrin degradation products. The BUN and CRTNN levels were elevated, which was considered to be related to the administration of diuretics. The serum UA and K levels were also elevated; the serum K was 5.6 mEq/L. Furthermore, the serum levels of LDH, GOT, and GPT were elevated. Serum CPK was slightly increased. Serum CRP was increased to 4.56 mg/dL. Thyroid functions were normal. The serum concentration of digoxin was slightly high. BNP was revealed to be considerably elevated to 5,410.8 pg/mL.

Dr. Ogawa: Will you please explain the reason for the distended jugular vein observed in this patient on admission?